**ORIGINAL ARTICLE**
Iran J Allergy Asthma Immunol
April 2025; 24(2):237-253.
DOI: 10.18502/ijaai.v24i2.18150

# Prognostic and Immunotherapeutic Value of Regulatory T Cell Marker Gene Signature in Melanoma

**Yurong Liu[1], Jianlan Liu[2], Keyu Jiang[3], Xiaolong Cheng[3], Sitong Di[3], Jian Tang[3], and Binlin Luo[3,4]**

[1] *The First Clinical Medical College, Nanjing Medical University, Nanjing, China*
[2] *Department of Orthopedics, The First Affiliated Hospital of Nanjing Medical University, Nanjing, China*
[3] *Department of Plastic and Burns Surgery, The First Affiliated Hospital of Nanjing Medical University, Nanjing, China*
[4] *Jiangsu Province (Suqian) Hospital, Suqian, China*

***Received: 28 October 2024; Received in revised form: 7 December 2024; Accepted: 18 December 2024***

## ABSTRACT

Regulatory T cells (Tregs) are central to establishing an immunosuppressive tumor microenvironment (TME), which promotes cancer progression and influences therapeutic outcomes. However, the prognostic significance of Treg-related genes (TRGs) in predicting immunotherapy response in melanoma remains insufficiently characterized. This study seeks to elucidate the role of TRGs in the antitumor immune response of melanoma.

The ordinary transcriptome and single-cell RNA sequencing (scRNA-seq) data were obtained from the gene expression omnibus and the cancer genome atlas databases. A multi-tiered quality control process was applied to scRNA-seq data, followed by cell annotation, cell-cell communication, and enrichment analysis to investigate Treg function in the melanoma microenvironment. Weighted gene coexpression network analysis (WGCNA) was employed to identify modules associated with Treg infiltration.

Key prognostic genes were identified using univariate Cox regression analysis and integrated into a prognostic model through least absolute shrinkage and selection operator and stepwise regression methods. The analysis revealed a Treg-related gene signature (TRGS) comprising *CHD3, FOSB, SEMA4D, PSME1, FYN, PRKACB*, and *ARID5A*. Higher TRGS-based risk scores were significantly associated with worse prognoses, immune cell infiltration, and stromal scores.

TRGS was identified as an independent prognostic indicator for melanoma, offering novel insights into the role of Tregs in modulating the TME. This study highlights the potential clinical utility of TRGs in melanoma diagnostics and personalized immunotherapy, providing a robust foundation for future therapeutic strategies.

**Keywords:** Immunotherapy; Melanoma; Regulatory T cell; Single cell sequencing; Tumor microenvironment

**Corresponding Authors:** Binlin Luo, MD;
Department of Plastic and Burns Surgery, The First Affiliated Hospital of Nanjing Medical University, Nanjing, China. Tel: (+86 138) 1386 5342, Fax: (+86 025) 6830 5392, Email: luobin8212192340@sina.com

Yurong Liu and Jianlan Liu contributed equally to this study.

Jian Tang, MD;
Department of Plastic and Burns Surgery, The First Affiliated Hospital of Nanjing Medical University, Nanjing, China. Tel: (+86 159) 5052 4693, Fax: (+86 025) 6830 5392, Email: tangjian@njmu.edu.cn

Copyright © 2025 Liu et al. Published by Tehran University of Medical Sciences.

This work is licensed under a Creative Commons Attribution-NonCommercial 4.0 International license (https://creativecommons.org/licenses/by-nc/4.0/). Non-commercial uses of the work are permitted, provided the original work is properly cited.

## INTRODUCTION

Melanoma, a highly aggressive skin tumor, poses significant risks for individuals, contributing to elevated mortality rates.[1] In 2020, there were 325 000 newly diagnosed cases of melanoma and 57 000 deaths attributed to the disease. If this trend continues, it is projected that by 2040, the number of new melanoma cases will increase by 50%, reaching 510 000, while the number of deaths will rise by 68%, totaling 96 000.[2] This malignancy exhibits a strong propensity for metastasis, often spreading to nearby subcutaneous tissues, regional lymph nodes, and distant organs, with the lung, brain, and liver being the most frequent sites of metastasis.[3] The median survival for patients with metastatic melanoma is between 6 and 9 months, and the 5-year survival rate remains under 5%.[4] In recent years, advancements in melanoma treatment have emerged with the development of molecular targeted therapies and immunotherapies. However, the effectiveness of traditional therapies is often compromised by treatment resistance and adverse toxicities. Combination therapies, in particular, are associated with more severe toxicities, frequently leading to treatment discontinuation.[5,6] Furthermore, the durability of treatment responses remains limited, with approximately 30% to 50% of melanoma patients experiencing disease progression within one year of treatment with immune checkpoint inhibitors or B-Raf proto-oncogene, serine/threonine kinase or mitogen-activated protein kinase inhibitors.[6,7] Therefore, uncovering the mechanisms behind melanoma progression is key to improving therapies and patient outcomes.

Regulatory T cells (Tregs) exhibit potent immunosuppressive properties, exerting both specific and nonspecific regulatory effects on the immune system.[8] They achieve immunosuppression by inhibiting dendritic cell maturation, secreting anti-inflammatory cytokines, and suppressing the activation and proliferation of antigen-specific effector T cells.[9] These functions are critical in preventing immune-mediated damage to self-tissues, thereby promoting immune tolerance and maintaining homeostasis.[10] Accumulating evidence has highlighted the pivotal role of Tregs in various pathological conditions, including autoimmune diseases and organ transplant rejection.[11,12] In the context of cancer, the immunosuppressive activity of Tregs has been associated with poorer clinical outcomes in cancer patients, where increased Treg infiltration in both the tumor microenvironment (TME) and peripheral blood suggests their involvement in cancer progression.[13,14]

Tregs, recognized as key players in maintaining immune tolerance, hold significant clinical relevance in melanoma due to their role in tumor-induced immunosuppression. Immunosuppression is a critical mechanism by which tumors evade immune surveillance, and the involvement of Tregs contributes to therapeutic resistance in progressive melanoma. Although the detailed cellular and molecular pathways of Treg-induced immunosuppression remain incompletely understood, both contact-dependent and independent mechanisms have been identified.[15] Increased frequencies of Tregs have been observed in various malignancies, including melanoma, where their presence is notable in the peripheral blood, local tumor microenvironment, and lymph nodes with metastases. The progression of melanoma has been shown to correlate with higher Treg frequencies, which in turn are associated with diminished immune responses following dendritic cell-based cancer therapies. These findings suggest a tumor-induced systemic suppression of T cell reactivity driven by increased Treg activity, which may partially explain the limited success of dendritic cell-based immunotherapies in advanced melanoma cases.[16]

Targeting Tregs represents a promising therapeutic strategy, and a deeper understanding of Treg-related genes (TRGs) and the molecular mechanisms of Treg-mediated immunosuppression is essential for the development of more effective treatments for melanoma.

Therefore, this study aimed to leverage single-cell RNA sequencing (scRNA-seq) data to investigate the role of classical immunosuppressive Tregs within the TME of melanoma, with a focus on identifying key TRGs. These TRGs were subsequently utilized to develop risk factors for predicting melanoma prognosis. Additionally, a comprehensive analysis was performed to explore the molecular characteristics associated with TRGs and their clinical significance. This study offers a novel perspective on the prognostic stratification of melanoma, contributing to the advancement of personalized treatment strategies and the improvement of clinical outcomes for melanoma patients.

## MATERIALS AND METHODS

### Data Source

To obtain relevant melanoma data, we accessed RNA expression profiles, immune profiles, and clinical survival data from the cancer genome atlas (TCGA) database via the University of California Santa Cruz (UCSC) Xena platform (https://xenabrowser.net). The inclusion criteria required that patients had a confirmed diagnosis of melanoma and possessed complete mRNA data along with comprehensive clinical information. Altogether, the clinical information and mRNA data of 450 individuals, who satisfied the selection criteria, were downloaded for further research. Additionally, independent external validation datasets (GSE19234, GSE22153, and GSE65904) were retrieved from the GEO database.[17–19] The raw data from all 4 datasets underwent background correction, normalization, and log2 transformation using the `affy` package. For genes recognized by multiple probes, the average probe value was calculated to estimate gene expression. To mitigate potential batch effects arising from dataset integration, the `sva` R package was employed for batch effect correction.

### Data Processing

For the analysis of melanoma scRNA-seq data (accession ID: GSE115978),[20] high-quality cells were retained by selecting those with fewer than 10% mitochondrial gene content and expressing more than 200 genes. Genes with expression levels between 200 and 7000, active in at least 3 cells, were included. Data integration was performed using the `Seurat` R package. The remaining cells were normalized and scaled through a linear regression model applying the "Log-normalization" method, and the top 2000 highly variable genes were identified using the `FindVariableFeatures` function. Dimensionality reduction was achieved through principal component analysis (PCA) and t-distributed stochastic neighbor embedding (t-SNE). To correct batch effects, soft k-means clustering was applied using the `harmony` package. Cell cycle heterogeneity within clusters was assessed using cell cycle markers embedded in the Seurat package. Clustering of cells was performed with the `FindClusters` function, applying a resolution parameter of 0.5. Cluster annotation was based on the identification of genes with elevated or unique expression patterns and recognized canonical markers. Finally, cell clustering results were visualized using the `Dimplot` function to assess the effectiveness of the clustering process.

### Cell Communication Analysis

To explore cell-cell communication between Tregs and other cell types within the TME, along with the activation of specific signaling pathways, we utilized the `CellChat` package.[21] `CellChat` assigned a probability value to each interaction and employed a permutation test to identify biologically significant cell-cell communications. Communication probabilities were estimated by integrating gene expression data with established ligand-receptor-cofactor interactions, modeled according to the law of mass action. Based on the inferred cell-cell communication network, we applied various visualization and quantitative analysis techniques to identify key signal senders (sources) and receivers (targets) within the signaling pathways. This allowed us to pinpoint signals that notably affected the outgoing or incoming communication of specific cell populations, providing critical insights into the main contributors to cell communication in the TME.[21,22] Additionally, we conducted enrichment analysis using the gene set "c2.cp.kegg.v7.4.symbols" from the MSigDB database as the reference dataset to further investigate the functional relevance of these signaling pathways.[23]

### Weighted Gene Coexpression Network Analysis

Weighted gene coexpression network analysis (WGCNA) was utilized to identify gene sets and expression patterns strongly correlated with Tregs in the bulk-transcriptome sequencing data.[24] In this analysis, a scale-free topology model was adopted, with the minimum soft-threshold power set at 0.8 or higher. The `ConstructNetwork` function was then applied to build the coexpression network based on the selected soft-threshold. Module eigengenes (ME) were subsequently calculated using the ModuleEigengenes function, which performed PCA on the gene expression matrix for each module, allowing for the identification of key module-specific genes.

### Acquisition and Verification of TRGs

From the aforementioned analyses, 2 gene sets were obtained: the module genes identified via WGCNA and the Tregs marker genes derived from single-cell subgroup analysis. To identify hub TRGs, we performed an intersection of these 2 gene sets, with the results

visualized using a Venn diagram. These intersecting genes were subsequently employed in machine learning models, facilitating a deeper understanding of the relationship between gene expression patterns, Tregs, and their roles in melanoma progression.

**Construction of the TRG Prognostic Model**

We analyzed the association between TRGs and melanoma through survival analysis, identifying genes significantly linked to prognosis. These genes were incorporated into a least absolute shrinkage and selection operator (LASSO) regression model using the `glmnet` R package to build a prognostic model.[25] The TCGA cohort served as the training set, while the GEO cohorts (GSE19234, GSE22153, GSE65904) were used for validation. Seven survival-related genes were selected for further analysis. The risk score formula was: risk score $= \sum_{i=1}^{n} \beta i * (\text{expression of gen}i)$, where β represents the regression coefficients and gene expression levels.

**Assessing the Independent Prognostic Value of the Risk Model**

To assess the robustness and predictive accuracy of the TRGs signature (TRGS), we employed PCA, Kaplan-Meier (KM) analysis, and receiver operating characteristic (ROC) curves. PCA illustrated patient stratification by TRG expression, while KM analysis categorized patients into high- and low-risk groups based on the median expression values across all cohorts, with statistical validation via the logrank test. ROC-AUC analysis was performed to evaluate model performance, using the area under the curve (AUC) values to measure diagnostic accuracy. This comprehensive analysis delineated the efficacy of the TRGS in prognostic predictions, showcasing its reliability and accuracy.

**Developing a Novel Nomogram**

A nomogram was developed to predict melanoma prognosis, incorporating the risk score and clinicopathological factors. Univariate and multivariate Cox regression analyses were used to determine significant variables ($p < 0.05$) for inclusion in the model. The accuracy of the nomogram was evaluated through calibration curves. Besides, to verify the universality, we conducted a stratified analysis to further evaluate the risk model's predictive capacity in each clinical subgroup. The modeling gene expression profiles and clinical characteristics were visualized with a heatmap.

**Immune correlation analysis of the model**

We employed seven distinct immune infiltration algorithms to thoroughly assess immune cell composition across different risk groups.[26,27] Heatmaps were utilized to visually represent the variations in immune cell infiltration, highlighting subtle differences between cell populations in these groups. Enrichment scores for 29 immune-related traits were calculated using single-sample gene set enrichment analysis (ssGSEA), while box plots were used to investigate differences in immune checkpoint gene expression between high- and low-risk groups. Additionally, the `estimate` R package was applied to compute immune scores, stromal scores, and ESTIMATE scores, enabling a comprehensive assessment of the TME. To evaluate the sensitivity to immunotherapy, immunophenoscores (IPS) were extracted from the TCGA-SKCM dataset within the Cancer Immunome Atlas (TCIA) database. This comprehensive immune profiling aimed to elucidate the relationship between the TRGS, immune cell infiltration, and potential responses to immunotherapy in melanoma patients.

**Drug Sensitivity Analysis Guided by TRGS**

To identify potentially effective chemotherapeutic agents across different risk groups, we employed the predictive capabilities of the `oncoPredict` R package.[28] This analysis enabled the determination of patients likely to demonstrate drug resistance or sensitivity, offering critical insights for the development of personalized treatment strategies.

**Statistical Analysis**

Data processing, statistical analysis, and graph plotting were conducted using R software, version 4.2.1. Spearman's correlation coefficients were used to evaluate relationships between continuous variables, while chi-square tests were applied for comparisons of categorical data. Depending on the data distribution, continuous variables were analyzed using either Wilcoxon rank-sum tests or Student's *t* tests. Parameters for the R packages were specified in the relevant sections, with default settings applied unless otherwise noted. All tests were 2-sided, with a significance level set at $p < 0.05$.

## RESULTS

### Single-cell Sequencing Reveals Unique TME Features in Melanoma

In the GSE115978 dataset, after removing low-quality cells, we retained 6,879 cells and 22,452 genes for analysis. Utilizing the `FindVariableFeatures` function, 2000 highly variable genes were selected for further exploration. PCA was applied for dimensionality reduction, followed by t-SNE using the first 30 principal components, which identified 15 distinct cell subsets (Figure 1A). By employing various annotation methods, we successfully classified these into 7 major cell types, including B cells, endothelial cells, epithelial cells, Tregs, fibroblasts, NK/$CD8^+$ T cells, and myeloid/$CD4^+$ T cells (Figure 1B). Tregs were characterized by higher expression of genes like *TNFRSF4*, *FOXP3*, and *IL2RA* compared to other T and NK cells. Figure 1D illustrates the distribution of stromal, epithelial, Tregs, and T cells in melanoma based on specific marker genes. Figure 1E presents signaling pathway enrichment differences across cell types, while Figure 1C shows expression patterns during different cell cycle phases. Analysis of cell communication highlighted the interactions and pathways through which Tregs engage with other cells in the TME, showing strong associations with various cell types (Figures 1F–G).

To improve comparability between the TCGA and GEO datasets, batch effects across the 4 datasets were corrected. Figure 2A shows the sample distributions before and after batch effect removal, demonstrating a uniform distribution postnormalization, which confirmed the effectiveness of the process. Differential expression markers of Tregs were utilized to assess TCGA-SKCM samples via the ssGSEA algorithm, followed by the application of WGCNA to identify gene modules most indicative of Tregs activity. A correlation coefficient exceeding 0.9 (with a soft threshold of 6) was found to provide a robust foundation for constructing multiple gene modules (Figure 2B). Correlation and adjacency matrices of gene expression profiles were used to construct a topological overlap matrix (TOM), followed by the application of hierarchical average linkage clustering to identify gene modules. Modules were defined by a minimum of 100 genes per module and a similarity threshold of >0.25 for module merging (Figure 2C). Six gene modules were identified using a dynamic tree-cutting method, as visualized in the heatmap (Figure 2D). The blue module showed a strong negative correlation with Treg cell infiltration ($r = -0.93$, $p < 0.001$) (Figure 2E). Finally, the genes identified from scRNA-seq analysis were cross-referenced with those identified through WGCNA, resulting in 77 genes were extracted for further analysis. (Figure 2F).

### Identification of TRGS

To refine gene selection and reduce redundancy, we applied LASSO Cox regression analysis. After performing multivariate Cox regression, we used a stepwise method to identify the optimal lambda value through 10-fold cross-validation, which minimized the model's partial likelihood deviance (Figure 3A). As shown in Figure 3B, increasing lambda caused the regression coefficients of predictors to gradually approach zero. We ultimately identified seven genes for the risk signature: *CHD3*, *FOSB*, *SEMA4D*, *PSME1*, *FYN*, *PRKACB*, and *ARID5A* (Figure 3C). Risk scores were calculated for each sample based on gene expression and corresponding Cox regression coefficients, followed by Z-mean normalization to classify patients into high- and low-risk groups. PCA across four cohorts highlighted distinct separation of melanoma patients based on risk scores, demonstrating the model's ability to differentiate between high- and low-risk individuals (Figure 3D). Survival analysis validated the prognostic power of TRGS, with high-risk patients consistently showing poorer outcomes across multiple cohorts ($p < 0.001$, Figure 3E). Additionally, ROC curve analysis confirmed the model's strong predictive accuracy for melanoma prognosis at 1-, 3-, and 5-year intervals (Figure 3F).

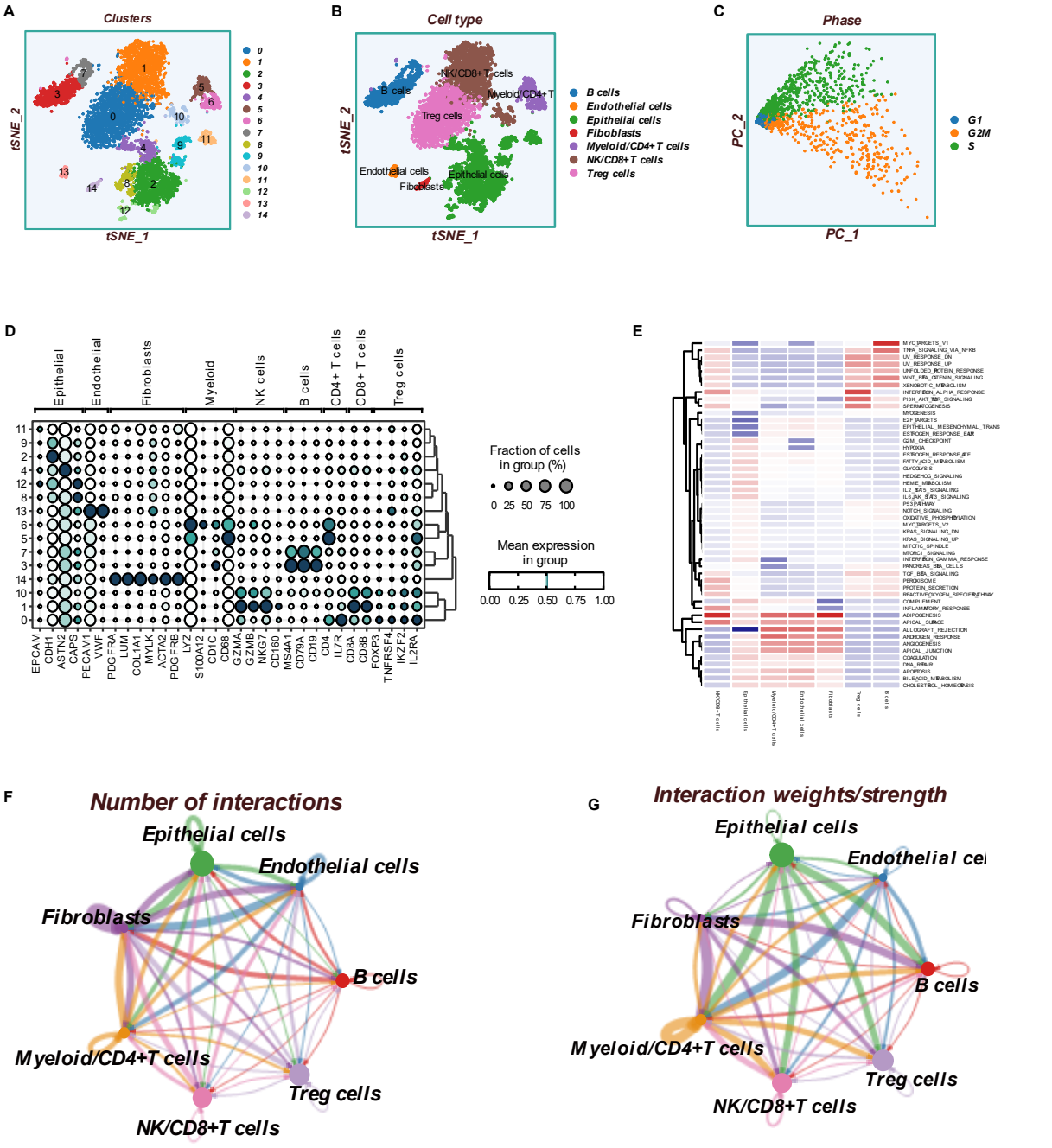


**Figure 1. Analysis of cell composition and function in melanoma samples. A. t-distributed stochastic neighbor embedding (t-SNE) plot displaying 15 distinct cell clusters. B. Seven cell types were identified based on marker gene expression. C. Principal component analysis (PCA) clustering was performed according to the cell cycle-related scores (G1, G2M, S-phase). D. Dot plots illustrating the expression of the top 3 marker genes across different cell types. E. Heatmap presenting enrichment analysis for each unique cell subtype. F–G. Variations in the number and strength of cellular communication across different cells.**

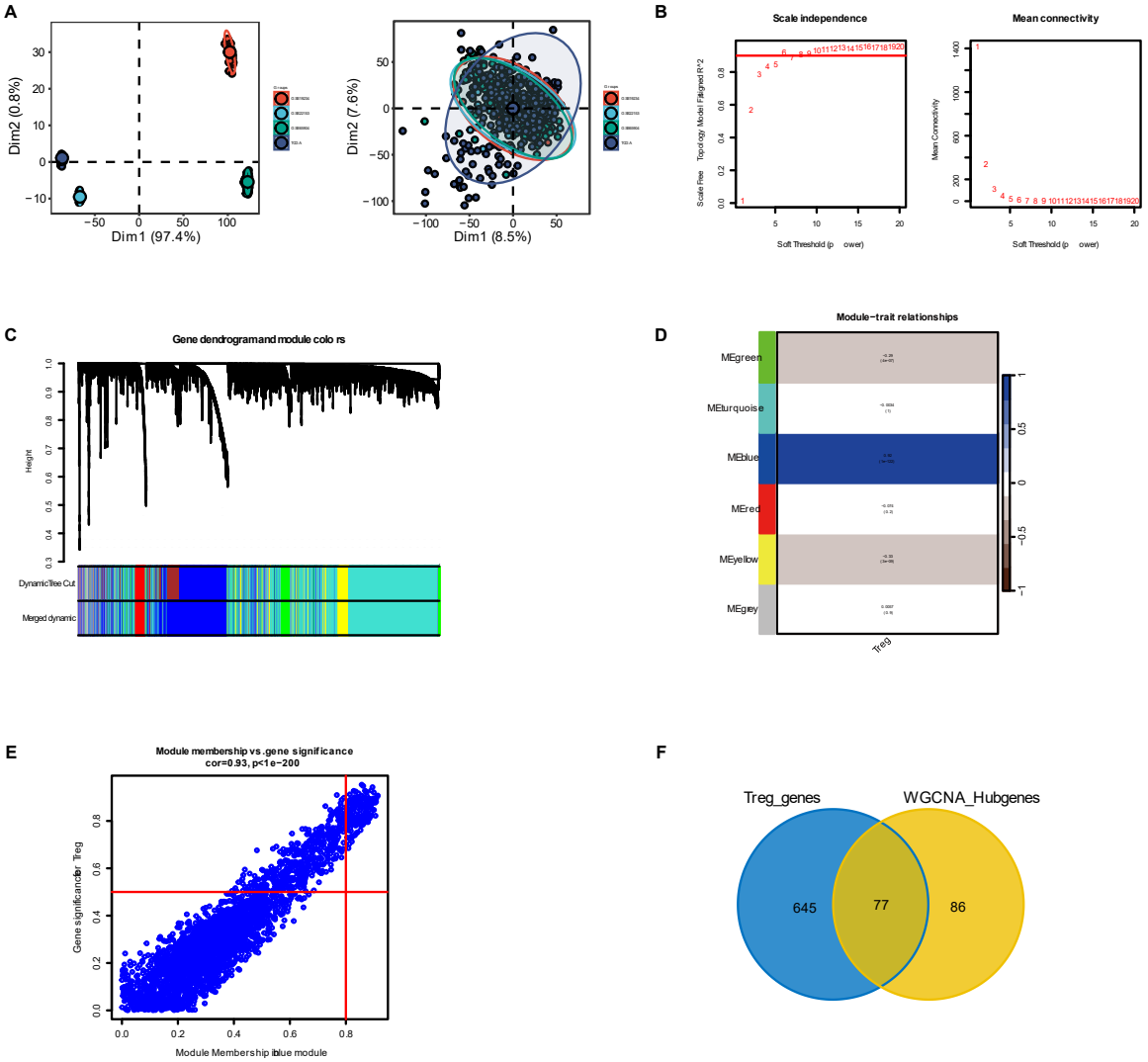


**Figure 2. Identification of Treg cell-related genes by weighted gene coexpression network (WGCNA). A. The batch effect between the cancer genome atlas (TCGA) cohort and 3 gene expression omnibus (GEO) cohorts was corrected. B. Selection of the optimal soft threshold (power) to ensure network consistency with scale-free topology. C. Coexpression network construction and gene clustering into modules. The top part shows the hierarchical clustering of genes, while the bottom highlights the gene modules. D. Heatmap showing the correlation between immune cell infiltration and gene modules. The first-row number represents the correlation coefficient, and the second row shows the *p* value. E. Correlation between the blue module and Tregs. F. Venn diagram showing the intersecting crucial genes identified by 2 methods.**

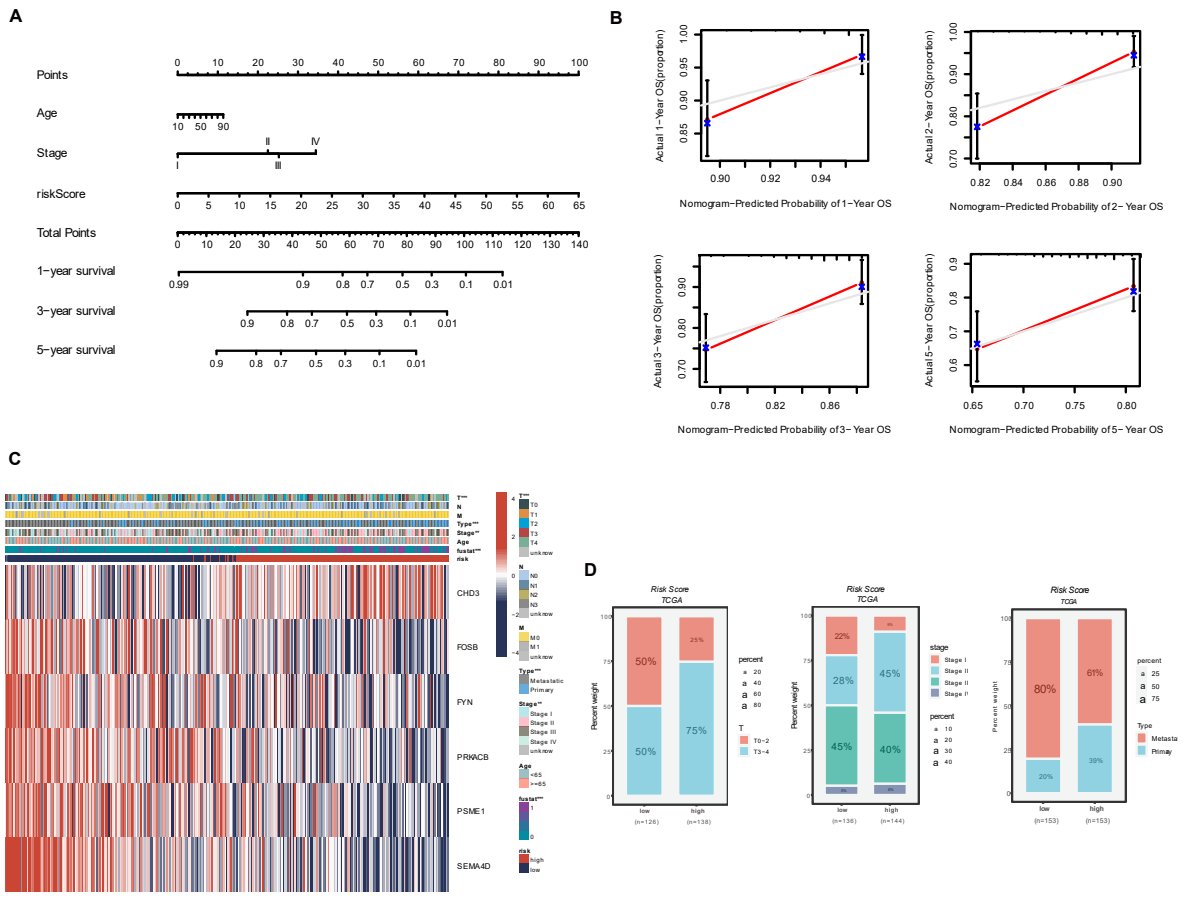


**Figure 3. Construction of Treg cell-related genes signature (TRGS). A–B. Optimal parameters for least absolute shrinkage and selection operator (LASSO) Cox regression were selected using 10-fold cross-validation. C. Forest plot visualizing the multivariate Cox coefficients for each gene in the TRGS. D. Principal component analysis (PCA) revealed a substantial divergence of the two risk groups. E. Survival curves of the TRGS regarding overall survival in the four datasets. F. Time-dependent receiver operating characteristic (ROC) curves of the TRGS regarding 1-, 3, and 5-year OS in the TCGA, GSE65904, GSE19234, and GSE22153 datasets.**

## Building a Nomogram with Better Predictive Performance

To improve the precision of TRGS, we combined clinicopathological factors with risk scores in univariate and multivariate Cox regression analyses to minimize redundancy and enhance accuracy. By integrating clinical stage, age, and risk score, we developed a nomogram to better predict melanoma patient outcomes (Figure 4A). Calibration curves confirmed the nomogram's reliability in forecasting 1-, 3-, and 5-year survival rates (Figure 4B). A heatmap was also generated to visualize clinical characteristics, highlighting significant differences between high- and low-risk groups in survival status, T stage, and clinical stage (Figure 4C). Patients with T3 or T4 melanoma had notably higher risk scores compared to those with T1 or T2. Additionally, the high-risk group had a higher proportion of stage II and III patients (Figures 4E–F). Our analysis confirmed a strong, independent association between the TRGS and melanoma prognosis.

## Immune Microenvironment Assessment

This investigation utilized data from 7 immune infiltration algorithms to evaluate immune infiltration disparities among distinct risk groups in the TCGA−SKCM cohort. The findings indicated enhanced immune infiltration levels within the low−risk group (Figure 5A).

Intriguingly, expression levels of model genes were positively correlated with most immune cell infiltration (Figure 5B). Employing the ssGSEA algorithm, further analysis of immune cell infiltration and function between the risk groups was conducted. Notably, melanoma patients in the low−risk group demonstrated elevated infiltration of various immune cells, including CD8+ T cells, $CD4^+$ T cells, dendritic cells, immature dendritic cells, neutrophils, and NK cells (Figure 5C). Through the ESTIMATE method, the study validated immune infiltration levels across different risk groups. Spearman correlation analysis revealed a negative correlation between risk score and immune score, suggesting that the degree of immune cell infiltration in the TME might account for the differences in disease progression and the efficacy of immunotherapy in melanoma patients (Figure 5E–F). Furthermore, the study examined the association between risk scores and well−known immune checkpoints in the TCGA−SKCM cohort, with the low−risk group exhibiting elevated expression of nearly all immune checkpoint genes (ICGs), including *PDCD1*, *IDO1*, *TIGIT*, and *LAG3* (Figure 5D). This observation provides crucial insights into the potential of immune checkpoint blockade therapy for melanoma patients. Conclusively, the study assessed the IPS across different risk groups to discern patients who might derive greater benefit from immunotherapy. The analysis showed that the low−risk subgroup had significantly higher IPS scores, indicating that those patients may benefit from immunotherapy (Figure 5G).

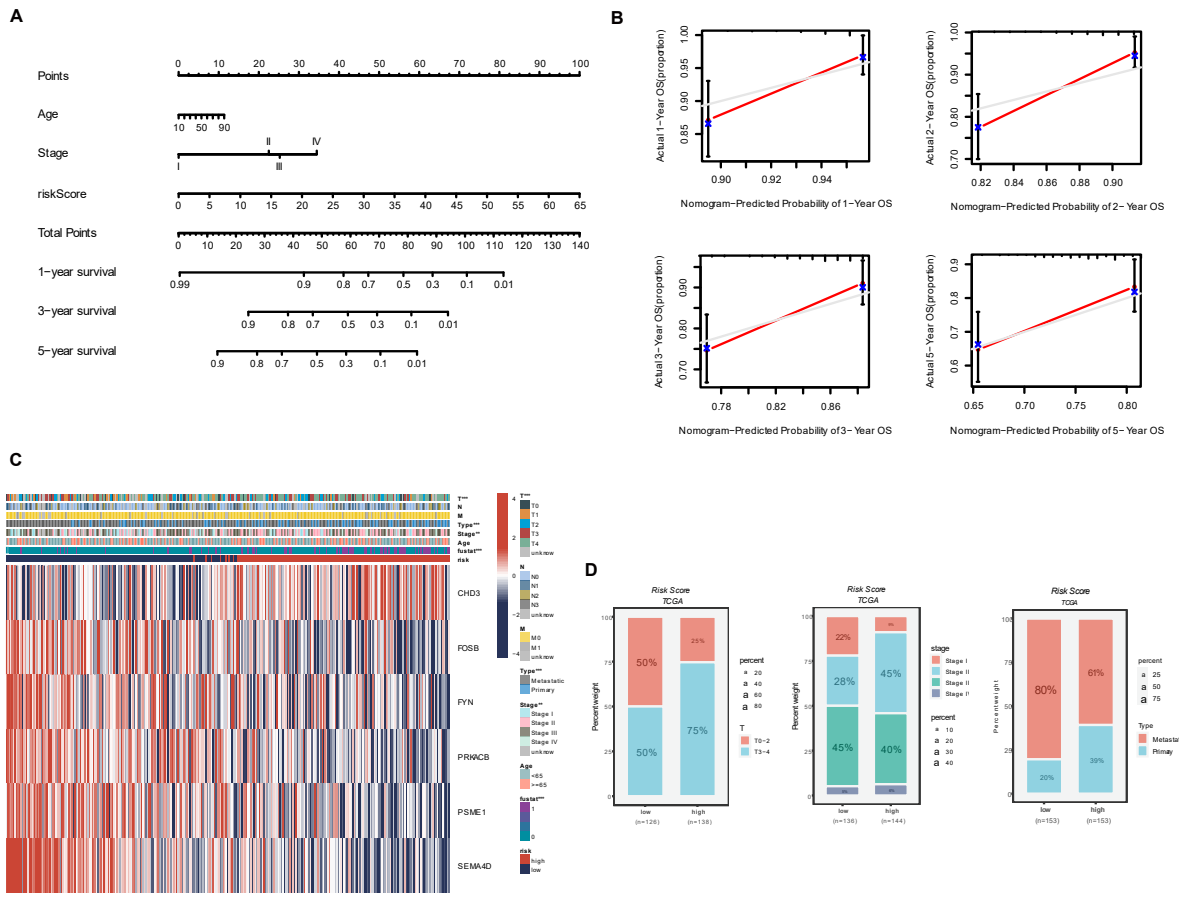


**Figure 4. Development of a nomogram integrating risk score. A. Nomogram construction, combining the T and N stages with the risk score. B. Calibration plots compare the actual and predicted overall survival rates, where the 45° line represents ideal prediction. C. Heatmap demonstrating differences in clinicopathological features between risk groups. T and stage differed significantly between groups. D. Distribution ratio of clinicopathological characteristics among different risk groups.**

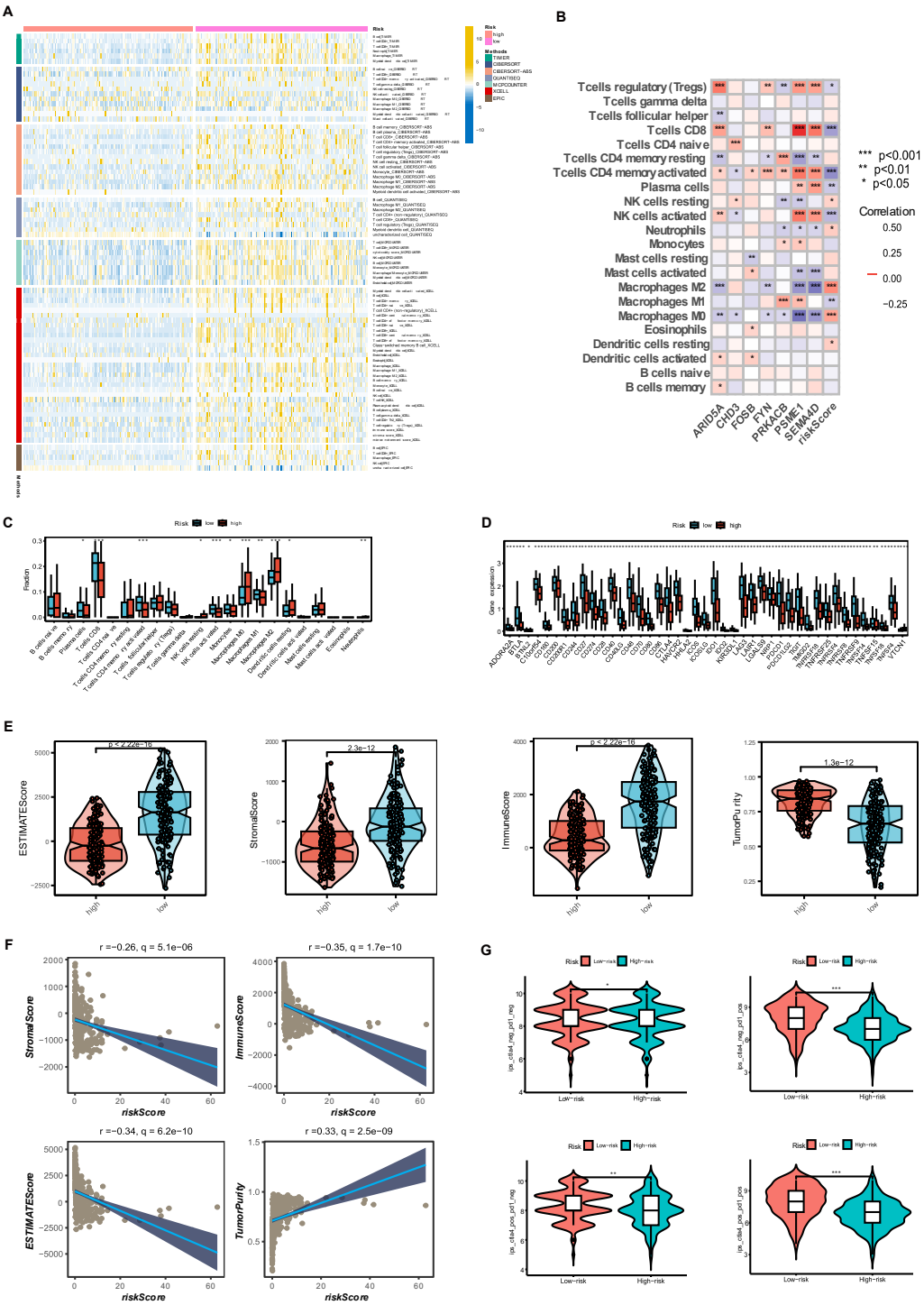


**Figure 5. Analysis of tumor microenvironment. A. Comparison of immune landscapes between high- and low-risk groups. B. Correlations between 7 hub genes and 22 immune-related cell types. C. Boxplot showing the difference of infiltration of 22 immune cells across risk groups. D. The expression of immune checkpoints genes across different risk groups. E. Differences in the stromal, immune, ESTIMATE, and tumor purity scores between the 2 risk groups. F. Correlation between risk score and stromal score, immune score, ESTIMATE score, and tumor purity. G. The cancer immunome atlas (TCIA) scores compared between high- and low-risk groups.**

**Drug Sensitivity**

Using `oncoPredict` drug sensitivity analysis, we identified potential therapeutic drugs for melanoma treatment based on TRGs in both risk groups. Patients with lower risk scores exhibited lower IC50 values for chemotherapeutic agents such as AUY922, Bosutinib, Camptothecin, and DMOG (Figure 6). These results highlight the utility of TRGs in predicting chemotherapy sensitivity, aiding in personalized treatment strategies for melanoma patients.

**Prognostic Significance of Key Model Genes**

The prognostic value of the 7 core genes was assessed. High expression levels of *ARID5A*, *FOSB*, *FYN*, *PRKACB*, *SEMA4D*, and *PSME1* were linked to better outcomes, while elevated *CHD3* expression was associated with poor prognosis. Univariate Cox regression confirmed that *CHD3* expression significantly correlated with OS and disease-specific survival in the TCGA cohort, as well as with OS in other datasets, including GSE98934, GSE22153, and GSE46517 (Figure 7I). Additionally, *CHD3* expression was predictive of drug resistance and sensitivity (Figure 7J), suggesting its complex role in both prognosis and treatment response in melanoma.

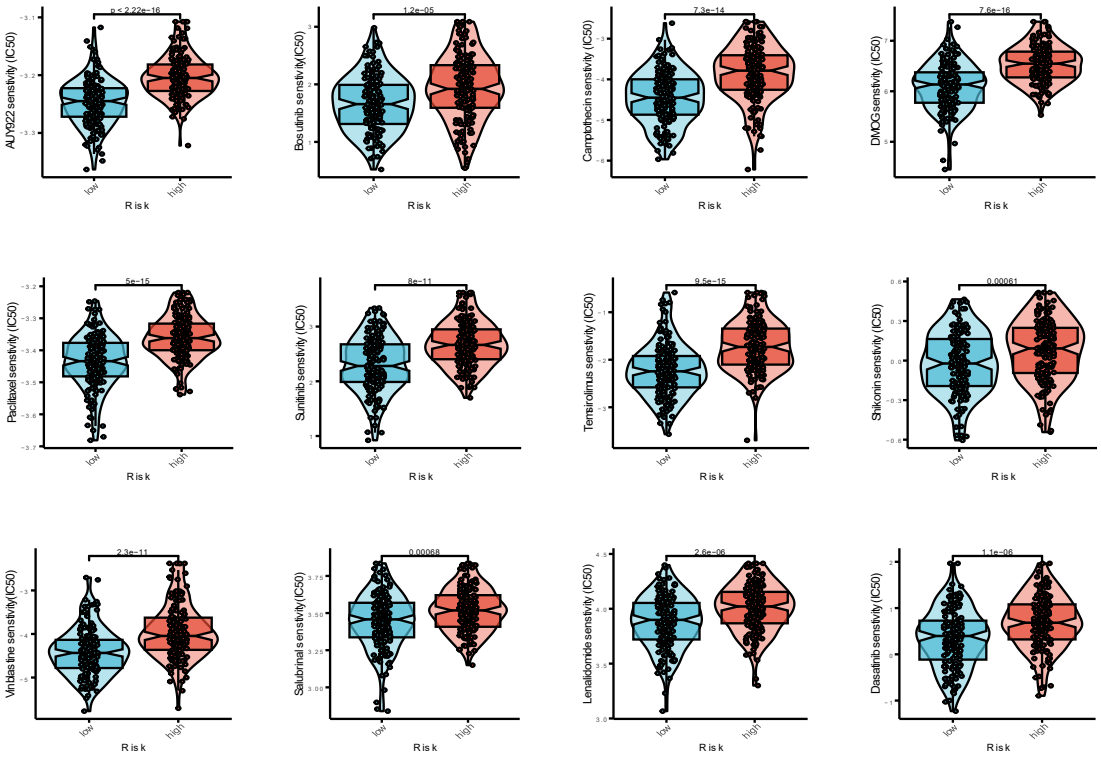


**Figure 6. Prediction of melanoma patients' sensitivity to chemotherapeutic drugs.**

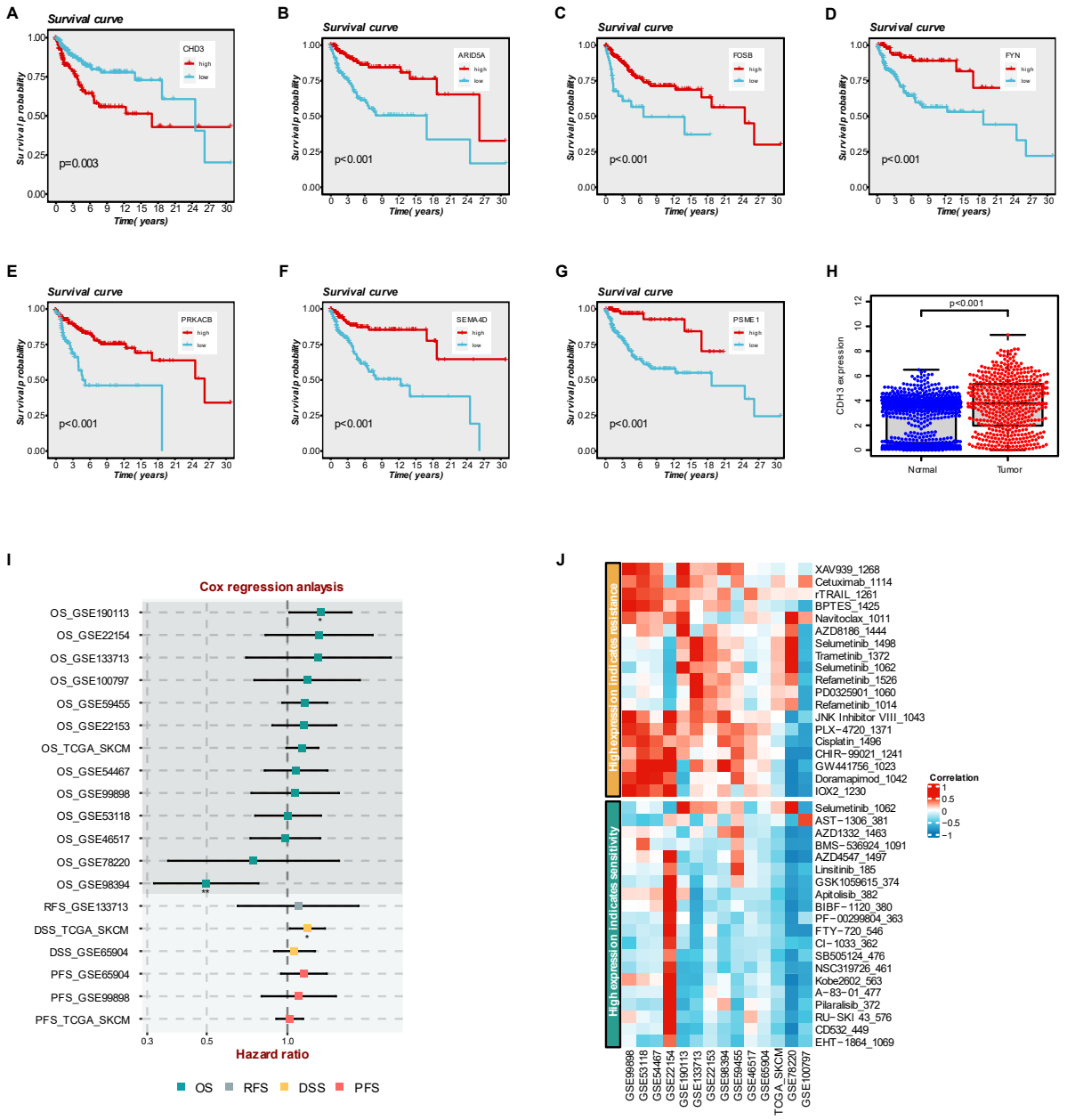


**Figure 7. Exploring the role of key gene *CHD3*. A–G. Survival analysis of 7 genes in TRGS. Patients with high *CHD3* expression had a significantly worse prognosis. C. *CHD3* was highly expressed in melanoma samples compared to the corresponding normal tissues of the genotype-tissue expression -skin dataset as a control. D. Univariate Cox regression analysis of different datasets. J. Drug sensitivity analysis of *CHD3*.**

## DISCUSSION

Tregs play a crucial role in maintaining immune balance by suppressing excessive autoimmune responses.[29] However, their function in tumor immunity is paradoxically suppressive. Increased infiltration of Tregs into tumor tissues is associated with a poorer prognosis in cancer patients.[10-12] Notably, tumor-derived Tregs exhibit stronger immunosuppressive activity compared to naturally occurring Tregs. Therefore, targeting Tregs in the TME presents a promising approach for improving cancer treatment outcomes.[30]

While modulating Tregs to fine-tune immune responses remains complex, recent studies have increasingly focused on the alterations in Tregs within melanoma. Nevertheless, there is a significant lack of research investigating the specific roles and diagnostic potential of Treg subsets in melanoma. This highlights the need for further detailed research to clarify the implications of Treg subpopulations for tumor diagnosis and therapeutic strategies.

In this investigation, scRNA-Seq was utilized to depict seven unique cellular phenotypes. The Treg population was identified based on their characteristic marker genes, followed by a differential gene expression analysis that uncovered 722 Treg-associated genes. This investigation revealed a strong connection between Tregs and the communication and specialization of various immune cells, as well as their impact on signaling pathways at the single-cell level. Additionally, WGCNA was employed to analyze bulk RNA-Seq data from melanoma samples, identifying gene modules closely related to Treg scores. In total, 77 genes were found to be associated with Tregs and demonstrated prognostic significance. The alignment of findings from both approaches reinforces the robustness of our results and enhances the overall understanding of Tregs in melanoma.

Furthermore, the development of a prognostic model using machine learning algorithms marked a notable advancement in predicting clinical outcomes for melanoma patients. Prognostic evaluations revealed that individuals in the high-risk group had a poorer prognosis. Our analysis identified seven key genes—*CHD3*, *FOSB*, *SEMA4D*, *PSME1*, *FYN*, *PRKACB*, and *ARID5A*—that were strongly associated with melanoma prognosis, showing direct correlations with Treg cell infiltration and contributing to disease progression. The TRGS demonstrated high accuracy and consistent performance across 3 additional public GEO datasets, as confirmed by ROC analysis, offering valuable insights into patient risk stratification over different time frames. By integrating clinical data, a nomogram was constructed to enhance predictive accuracy. The nomogram outperformed traditional risk scores and other clinical parameters in forecasting patient survival outcomes. The TME composed of various elements such as the extracellular matrix, tumor-infiltrating lymphocytes, and neo-angiogenesis, plays a crucial role in cancer immunotherapy.[31] Effective interventions targeting the TME can activate cytotoxic T cells in vivo, promoting tumor elimination. This study aimed to assess the significance of immune infiltration in tumors by comparing immune cell infiltration between high- and low-risk patient groups. Results indicated that low-risk tumors exhibited higher immune cell infiltration, as shown by the immune infiltration algorithm, with further confirmation from the ESTIMATE algorithm. A negative correlation between immune scores and risk scores suggested that tumors in the low-risk group had significantly more immune cell infiltration. Additionally, an analysis of immune checkpoint expression, including *PDL1* and *CTLA4*, revealed higher expression levels in the low-risk group. Most immune checkpoint genes were inversely correlated with the risk score, further highlighting the differences between the 2 groups.

Immunotherapy has emerged as a promising approach in melanoma treatment by targeting the tumor's immune evasion mechanisms and activating the patient's immune system to attack cancer cells.[18,30] However, its effectiveness varies between individuals, making it essential to implement thorough screening and evaluation protocols to determine the suitability of immunotherapy for each patient.[32] The introduction of PD-1/PD-L1 inhibitors has opened new possibilities and challenges in melanoma therapy.[33] To evaluate differences in immunotherapy responses between risk groups, we utilized TCIA to examine the effects of PD-1 and CTLA-4 treatments. The IPS scores of low-risk melanoma patients were significantly higher than those of high-risk patients, suggesting that individuals in the low-risk group may benefit more from immunotherapy. We aim for PD-1/PD-L1 inhibitors to play a key role in adjuvant therapy for newly diagnosed high-risk melanoma, providing surgeons with more accurate treatment strategies through relevant clinical studies. Ultimately, our goal is to improve patient outcomes and enhance quality of life by refining therapeutic approaches.

Our study has identified seven key genes that are strongly associated with melanoma prognosis, and we have shown that these genes have direct correlations with Treg cell infiltration, which contributes to disease progression. Among these seven candidate genes constituting the prognostic model, *CHD3* has been implicated in chromatin remodeling, and we observed that *CHD3* was significantly highly expressed in the melanoma high-risk population, which correlates with increased metastatic potential and poor prognosis.[34,35]

FOSB, a member of the AP-1 transcription factor family, was significantly higher in older melanoma patients with positive sentinel lymph node status, aligning with its known oncogenic role.[36] PSME1 not only balanced proteasome function but also correlated with multiple malignancies and acted as a prognostic predictor. Consistently, we observed high expression of PSME1 is associated with a favorable prognosis and may act as potential prognostic biomarkers in melanoma, which is consistent with previous reports.[37] ARID5A was a dynamic molecule that was translocated to the cytoplasm and stabilizes a variety of inflammatory mRNA transcripts, including IL-6, STAT3, OX40, T-bet, and IL-17-induced targets, and contributes to the inflammatory response.[38] *ARID5A* regulates inflammation and cytokine pathways, contributing to immune escape mechanisms in various cancers.[39] Besides, higher *SEMA4D* expression was significantly correlated with a better prognosis of melanoma. Importantly, *SEMA4D* expression positively correlated to the immune infiltrating levels and diverse immune markers in various tumors, suggesting that SEMA4D might participate in immune regulation of cancers.[40] In addition, *FYN* is highly expressed in melanoma cells and clinical samples, and the knockdown of *FYN* expression significantly suppresses the malignant phenotype of melanoma cells. This phenomenon suggested a critical role of the FYN/CD147 signaling axis in the invasion and metastasis of melanoma cells and deemed it a potential therapeutic target for melanoma therapy.[41] PRKACB, involved in protein kinase A signaling, is known to promote tumor growth and therapy resistance in glioblastoma,[42] but its role in melanoma has not yet been elucidated.

LASSO regression is known to remove unimportant variables via the regression coefficients penalizing the size of the parameters. LASSO penalizes the regression variable coefficient and shrinks it to zero. After that, it selects the variables with non-zero coefficients for constructing the model.[43] The present work demonstrated the potential use of this approach for developing predictive models for the early diagnosis of other cancers. While LASSO is effective in handling high-dimensional data and selecting relevant features by applying regularization, it may not always account for complex interactions between features. LASSO assumes linear relationships between variables, which might not capture the full complexity of biological systems. Additionally, its performance can be sensitive to the choice of regularization parameter, which may require careful tuning to avoid overfitting or underfitting the model.[44,45] WGCNA is a powerful tool for both data exploration and gene screening. It allows for the identification of modules (gene clusters) within a network and provides insights into gene-module relationships, such as module membership and eigengene networks.[46] WGCNA can also be used to rank genes or modules based on their correlation with sample traits, facilitating the generation of testable hypotheses for further validation in independent datasets. However, it is primarily based on pairwise correlations, which may overlook more complex dependencies and nonlinear relationships between genes. The method also assumes that coexpression modules are biologically relevant, which may not always hold true. Moreover, although several coexpression module detection methods are implemented, the package does not provide the means to determine which method is best. The accuracy of the network construction can be affected by the choice of soft-thresholding power, which can influence the identification of modules.[47-49]

While the bioinformatics analyses presented in this study offer valuable insights, there are several limitations to consider. First, our study relies on publicly available datasets, which may introduce biases or inconsistencies inherent in such data, including issues related to sample heterogeneity, data quality, and potential confounders. Although we have implemented rigorous preprocessing and normalization steps to minimize these concerns, the nature of publicly accessible datasets can still impose some limitations on the generalizability of the findings. Additionally, the lack of experimental validation of our bioinformatic predictions represents another limitation. While the bioinformatics analyses presented here provide valuable insights into the role of Treg marker genes in melanoma. However, due to resource constraints, we were unable to perform such experiments within the timeframe and scope of this study. We therefore encourage future research to validate our findings through appropriate experimental models, as this would offer critical confirmation and help further elucidate the biological significance of our predictions. Besides, while our bioinformatic analyses suggest that the TRGS model holds promise as a prognostic tool, further validation in prospective clinical trials is essential to confirm its clinical utility. Future studies should aim to involve diverse patient populations across different clinical

settings to assess the model's predictive power and its potential application in personalized medicine. Such clinical validation would also help to address any potential biases introduced by retrospective dataset analysis and ensure that the model's performance is consistent across various demographic groups. Nonetheless, the integrated analysis and use of machine learning provided valuable insights into the prognostic role of Tregs in melanoma and their potential therapeutic applications.

In conclusion, our study advances the understanding of Tregs in melanoma by highlighting their pivotal role in shaping the TME, modulating immune responses, and serving as a prognostic marker. By integrating bulk and scRNA-seq, machine learning models, and immune correlation analysis, we provide a comprehensive view of Tregs dynamics in melanoma. These insights lay the groundwork for developing targeted therapeutic strategies and personalized medicine approaches to better combat this aggressive cancer.

## STATEMENT OF ETHICS

This study was conducted in accordance with the ethical standards outlined in the Declaration of Helsinki. All data used in this research were obtained from publicly available databases, including TCGA and GEO, and no direct involvement of human participants or animals was required. Therefore, additional ethical approval or informed consent was not necessary for this study. The use of these datasets complies with the terms and conditions set by their respective platforms.

## FUNDING

This study did not receive any funding in any form.

## CONFLICT OF INTEREST

The authors declare no conflicts of interest.

## ACKNOWLEDGMENTS

We are very grateful for the data provided by databases such as TCGA and GEO.

## DATA AVAILABILITY

Upon reasonable request from the corresponding author via tangjian@njmu.edu.cn.

## AI ASSISTANCE DISCLOSURE

Not applicable.

## REFERENCES

1. Long GV, Swetter SM, Menzies AM, Gershenwald JE, Scolyer RA. Cutaneous melanoma. Lancet. 2023;402(10400):485-502.
2. Liu J, Pei S, Zhang P, Jiang K, Luo B, Hou Z, et al. Liquid-liquid phase separation throws novel insights into treatment strategies for skin cutaneous melanoma. Bmc Cancer. 2023;23(1):388.
3. Wang JY, Wang EB, Swetter SM. What Is Melanoma? Jama-J Am Med Assoc. 2023;329(11):948.
4. Michielin O, Atkins MB, Koon HB, Dummer R, Ascierto PA. Evolving impact of long-term survival results on metastatic melanoma treatment. J Immunother Cancer. 2020;8(2):e000948.
5. Robert C, Grob JJ, Stroyakovskiy D, Karaszewska B, Hauschild A, Levchenko E, et al. Five-Year Outcomes with Dabrafenib plus Trametinib in Metastatic Melanoma. New Engl J Med. 2019;381(7):626-36.
6. Wolchok JD, Chiarion-Sileni V, Gonzalez R, Grob JJ, Rutkowski P, Lao CD, et al. Long-Term Outcomes With Nivolumab Plus Ipilimumab or Nivolumab Alone Versus Ipilimumab in Patients With Advanced Melanoma. J Clin Oncol. 2022;40(2):127-37.
7. Dimitriou F, Long GV, Menzies AM. Novel adjuvant options for cutaneous melanoma. Ann Oncol. 2021;32(7):854-65.
8. Tay C, Tanaka A, Sakaguchi S. Tumor-infiltrating regulatory T cells as targets of cancer immunotherapy. Cancer Cell. 2023;41(3):450-65.
9. Li L, Yu R, Cai T, Chen Z, Lan M, Zou T, et al. Effects of immune cells and cytokines on inflammation and immunosuppression in the tumor microenvironment. Int Immunopharmacol. 2020;88:106939.
10. Moreno AM, Li Z, DuPage M. Treg programming and therapeutic reprogramming in cancer. Immunology. 2019;157(3):198-209.
11. Togashi Y, Shitara K, Nishikawa H. Regulatory T cells in cancer immunosuppression - implications for anticancer therapy. Nat Rev Clin Oncol. 2019;16(6):356-71.
12. Tanaka A, Sakaguchi S. Regulatory T cells in cancer immunotherapy. Cell Res. 2017;27(1):109-18.
13. Shan F, Somasundaram A, Bruno TC, Workman CJ,

Vignali D. Therapeutic targeting of regulatory T cells in cancer. Trends Cancer. 2022;8(11):944-61.
14. Harris RJ, Willsmore Z, Laddach R, Crescioli S, Chauhan J, Cheung A, et al. Enriched circulating and tumor-resident TGF-beta(+) regulatory B cells in patients with melanoma promote FOXP3(+) Tregs. Oncoimmunology. 2022;11(1):2104426.
15. Correll A, Tuettenberg A, Becker C, Jonuleit H. Increased regulatory T-cell frequencies in patients with advanced melanoma correlate with a generally impaired T-cell responsiveness and are restored after dendritic cell-based vaccination. Exp Dermatol. 2010;19(8):e213-21.
16. Noyes D, Bag A, Oseni S, Semidey-Hurtado J, Cen L, Sarnaik AA, et al. Tumor-associated Tregs obstruct antitumor immunity by promoting T cell dysfunction and restricting clonal diversity in tumor-infiltrating CD8+ T cells. J Immunother Cancer. 2022;10(5):e004605.
17. Jonsson G, Busch C, Knappskog S, Geisler J, Miletic H, Ringner M, et al. Gene expression profiling-based identification of molecular subtypes in stage IV melanomas with different clinical outcome. Clin Cancer Res. 2010;16(13):3356-67.
18. Bogunovic D, O'Neill DW, Belitskaya-Levy I, Vacic V, Yu YL, Adams S, et al. Immune profile and mitotic index of metastatic melanoma lesions enhance clinical staging in predicting patient survival. P Natl Acad Sci Usa. 2009;106(48):20429-34.
19. Cabrita R, Lauss M, Sanna A, Donia M, Skaarup LM, Mitra S, et al. Tertiary lymphoid structures improve immunotherapy and survival in melanoma. Nature. 2020;577(7791):561-5.
20. Jerby-Arnon L, Shah P, Cuoco MS, Rodman C, Su MJ, Melms JC, et al. A Cancer Cell Program Promotes T Cell Exclusion and Resistance to Checkpoint Blockade. Cell. 2018;175(4):984-97.
21. Jin S, Plikus MV, Nie Q. CellChat for systematic analysis of cell-cell communication from single-cell transcriptomics. Nat Protoc. 2024;
22. Jin S, Guerrero-Juarez CF, Zhang L, Chang I, Ramos R, Kuan CH, et al. Inference and analysis of cell-cell communication using CellChat. Nat Commun. 2021;12(1):1088.
23. Liberzon A, Subramanian A, Pinchback R, Thorvaldsdottir H, Tamayo P, Mesirov JP. Molecular signatures database (MSigDB) 3.0. Bioinformatics. 2011;27(12):1739-40.
24. Langfelder P, Horvath S. WGCNA: an R package for weighted correlation network analysis. Bmc Bioinformatics. 2008;9:559.
25. Engebretsen S, Bohlin J. Statistical predictions with glmnet. Clin Epigenetics. 2019;11(1):123.
26. Li T, Fu J, Zeng Z, Cohen D, Li J, Chen Q, et al. TIMER2.0 for analysis of tumor-infiltrating immune cells. Nucleic Acids Res. 2020;48(W1):W509-14.
27. Liu J, Pei S, Zhang P, Jiang K, Luo B, Hou Z, et al. Liquid-liquid phase separation throws novel insights into treatment strategies for skin cutaneous melanoma. Bmc Cancer. 2023;23(1):388.
28. Maeser D, Gruener RF, Huang RS. oncoPredict: an R package for predicting in vivo or cancer patient drug response and biomarkers from cell line screening data. Brief Bioinform. 2021;22(6):bbab260.
29. Iglesias-Escudero M, Arias-Gonzalez N, Martinez-Caceres E. Regulatory cells and the effect of cancer immunotherapy. Mol Cancer. 2023;22(1):26.
30. Chen BJ, Zhao JW, Zhang DH, Zheng AH, Wu GQ. Immunotherapy of Cancer by Targeting Regulatory T cells. Int Immunopharmacol. 2022;104:108469.
31. Xiao Y, Yu D. Tumor microenvironment as a therapeutic target in cancer. Pharmacol Therapeut. 2021;221:107753.
32. Kalaora S, Nagler A, Wargo JA, Samuels Y. Mechanisms of immune activation and regulation: lessons from melanoma. Nat Rev Cancer. 2022;22(4):195-207.
33. Kirkwood JM, Tarhini AA, Panelli MC, Moschos SJ, Zarour HM, Butterfield LH, et al. Next generation of immunotherapy for melanoma. J Clin Oncol. 2008;26(20):3445-55.
34. Zhao S, Allis CD, Wang GG. The language of chromatin modification in human cancers. Nat Rev Cancer. 2021;21(7):413-30.
35. Chang S, Yim S, Park H. The cancer driver genes IDH1/2, JARID1C/ KDM5C, and UTX/ KDM6A: crosstalk between histone demethylation and hypoxic reprogramming in cancer metabolism. Exp Mol Med. 2019;51(6):1-17.
36. Menefee DS, McMasters A, Pan J, Li X, Xiao D, Waigel S, et al. Age-related transcriptome changes in melanoma patients with tumor-positive sentinel lymph nodes. Aging (Albany NY). 2020;12(24):24914-39.
37. Wang Q, Pan F, Li S, Huang R, Wang X, Wang S, et al. The prognostic value of the proteasome activator subunit gene family in skin cutaneous melanoma. J Cancer. 2019;10(10):2205-19.
38. Nyati KK, Zaman MM, Sharma P, Kishimoto T. Arid5a, an RNA-Binding Protein in Immune Regulation: RNA Stability, Inflammation, and Autoimmunity. Trends Immunol. 2020;41(3):255-68.
39. Kang Z, Wang J, Huang W, Liu J, Yan W. Identification of Transcriptional Heterogeneity and Construction of a

Prognostic Model for Melanoma Based on Single-Cell and Bulk Transcriptome Analysis. Front Cell Dev Biol. 2022;10:874429.
40. Lu Q, Cai P, Yu Y, Liu Z, Chen G, Zeng Z. Sema4D correlates with tumour immune infiltration and is a prognostic biomarker in bladder cancer, renal clear cell carcinoma, melanoma and thymoma. Autoimmunity. 2021;54(5):294-302.
41. Liu C, Li S, Tang Y. Advances in the expression and function of Fyn in different human tumors. Clin Transl Oncol. 2023;25(10):2852-60.
42. Larriba E, de Juan RC, Garcia-Martinez A, Quintanar T, Rodriguez-Lescure A, Soto JL, et al. Identification of new targets for glioblastoma therapy based on a DNA expression microarray. Comput Biol Med. 2024;179:108833.
43. Ahmed F, Khan AA, Ansari HR, Haque A. A Systems Biology and LASSO-Based Approach to Decipher the Transcriptome-Interactome Signature for Predicting Non-Small Cell Lung Cancer. Biology-Basel. 2022;11(12):1752.
44. Frost HR, Amos CI. Gene set selection via LASSO penalized regression (SLPR). Nucleic Acids Res. 2017;45(12):e114.
45. Kang J, Choi YJ, Kim IK, Lee HS, Kim H, Baik SH, et al. LASSO-Based Machine Learning Algorithm for Prediction of Lymph Node Metastasis in T1 Colorectal Cancer. Cancer Res Treat. 2021;53(3):773-83.
46. Langfelder P, Horvath S. WGCNA: an R package for weighted correlation network analysis. Bmc Bioinformatics. 2008;9:559.
47. Horvath S, Dong J. Geometric interpretation of gene coexpression network analysis. Plos Comput Biol. 2008;4(8):e1000117.
48. Weston DJ, Gunter LE, Rogers A, Wullschleger SD. Connecting genes, coexpression modules, and molecular signatures to environmental stress phenotypes in plants. BMC Syst Biol. 2008;2:16.
49. Langfelder P, Zhang B, Horvath S. Defining clusters from a hierarchical cluster tree: the Dynamic Tree Cut package for R. Bioinformatics. 2008;24(5):719-20.